Microfabrication-based modulation of embryonic stem cell differentiation

Jaesung Park,[a] Cheul H. Cho,[a] Natesh Parashurama,[ab] Yawen Li,[a] François Berthiaume,[a] Mehmet Toner,[a] Arno W. Tilles[a] and Martin L. Yarmush*[ab]

Received 29th March 2007, Accepted 24th May 2007
First published as an Advance Article on the web 13th June 2007
DOI: 10.1039/b704739h

Embryonic stem (ES) cells form spontaneous aggregates during differentiation, and cell–cell communication in the aggregates plays an important role in differentiation. The development of a controlled differentiation scheme for ES cells has been hindered by the lack of a reliable method to produce uniform aggregate sizes. Conventional techniques, such as hanging drop and suspension cultures, do not allow precise control over size of ES cell aggregates. To surmount this problem, we microfabricated adhesive stencils to make mouse ES (mES) cell aggregates of specific sizes ranging from 100 μm to 500 μm in diameter. With this technique, we studied the effect of the initial aggregate size on ES cell differentiation. After 20 days of induction of differentiation, we analyzed the stem cell populations using gene and protein expression assays as well as biochemical functions. Notably, we found that germ layer differentiation depends on the initial size of the ES cell aggregate. Among the ES cell aggregate sizes tested, the aggregates with 300 μm diameter showed similar differentiation profiles of three germ layers as embryoid bodies made using the ''hanging drop'' technique. The smaller (100 μm) aggregates showed the increased expression of ectodermal markers compared to the larger (500 μm) aggregates, while the 500 μm aggregates showed the increased expression of mesodermal and endodermal markers compared to the 100 μm aggregates. These results indicate that the initial size of the aggregate is an important factor for ES cell differentiation, and can affect germ layer selection as well as the extent of differentiation.

Introduction

Embryonic stem (ES) cells promise to be useful therapeutically due to their ability to self-renew and differentiate into derivatives of all three major germ layers.[1–3] Currently, methods are available to differentiate ES cells into ectoderm,[4–6] mesoderm,[7–9] and endoderm[10] derivatives. During differentiation, ES cells form aggregates. In *in vitro* culture, ES cell aggregates called embryoid bodies (EBs) can be typically made by using the 'hanging drop' method.[11] Once these aggregates form, they keep proliferating and differentiating, recapitulating early development and germ layer formation. Extensive studies have been performed using differentiation directed by growth factors.[12–18] However, ES cells can also spontaneously form aggregates and differentiate without exogenous growth factors. This suggests that cell–cell interactions induce differentiation, most likely by mimicking the natural microenvironment and releasing autocrine factors.[19,20] The question of how these aggregates affect differentiation is poorly understood. For example, when ES cells are differentiated as single cells in a monolayer culture, differentiation into the hematopoietic lineage is repressed,[9,21,22] and differentiation into osteoblasts is dominant.[23] Also, when ES cells are differentiated as EBs, the EBs with an initial number of cells of ~1000 showed more hematopoietic differentiation, indicating ES cell differentiation may depend on the extent of initial cell–cell interaction.[24,25]

Microfabrication may offer advantages for studying ES cell biology because it can provide control of the cellular microenvironment. Reports have shown that microfabrication is effective in providing a high level of control over heterotypic cell–cell contact,[26,27] cell geometry,[28] cell differentiation,[29,30] and size of EB.[31,32] The majority of these studies were based on extracellular matrix (ECM) patterning or geometric constraint, such as a well, which later constrained differentiation and proliferation of ES cells. In contrast, the microfabricated stencil technique provides a homogeneous surface without constraint on cells,[33] thereby allowing cell outgrowth, and can be useful for studying ES cell differentiation.

In this study, we investigated the effect of the size of ES cell aggregates on differentiation through the use of a microfabricated stencil technique.[33] Using these microfabricated stencils, we controlled the initial sizes of the ES cell aggregate between 100 and 500 μm. We cultured them to investigate their differentiation without physical constraint. After 20 days of culture, we performed gene and protein expression studies. The results demonstrated that germ layer formation varied with the initial size of the aggregate. Among the aggregate sizes we tested, the aggregates with 300 μm diameter showed gene and protein expression profiles similar to EBs formed by the ''hanging drop'' technique with approximately 1000 cells and approximately 300 μm in diameter. This study indicates that initial aggregate size is a critical factor in ES cell differentiation.

[a]*Center for Engineering in Medicine and Surgical Services, Massachusetts General Hospital, Shriners Hospitals for Children and Harvard Medical School, GRB 1401, 55 Fruit Street, Boston, Massachusetts 02114, USA. E-mail: ireis@sbi.org; Tel: +1 617-371-4882*
[b]*Department of Biomedical Engineering, Rutgers University, Piscataway, NJ 08845, USA*

Material and methods

Cell culture and differentiation

Culture medium to maintain the ES cells in an undifferentiated state consisted of Knockout D-MEM supplemented with 15% (v/v) Knockout Serum Replacement (Invitrogen, Carlsbad, CA), 4 mM L-glutamine (Cambrex, Walkersville, MD), 100 μg mL^{-1} penicillin–streptomycin (Invitrogen), 10^3 U mL^{-1} leukemia inhibitory factor (LIF) (Chemicon, Temecula, CA), and 10 μg mL^{-1} gentamicin (Invitrogen), and 0.1 mM 2-mercaptoethanol (Sigma, St. Louis, MO). The tissue culture plates (T75) were coated with 0.1% gelatin (Sigma). ES-D3 cells (ATCC, Manassas, VA) and ES-R1 (Oct4-GFP, provided by Dr A. Nagy, Mount Sinai Hospital, Toronto, Ontario, Canada) were cultured in the non-differentiating medium at 37 °C, with medium changed daily. When the ES cells on the tissue culture plates were 80% confluent, they were detached using trypsin/EDTA (0.1%/1 mM), and transferred to new plates. Differentiation culture medium consisted of Iscove's Modified Dulbecco's Medium (Gibco, Gaithersburg, MD) supplemented with 20% (v/v) fetal bovine serum (Gibco, Gaithersburg, MD), 4 mM L-glutamine (Cambrex), 100 U mL^{-1} penicillin–streptomycin (Invitrogen), and 0.01 mg mL^{-1} gentamicin (Gibco).

For hanging drop EB formation, approximately 1000 ES cells were suspended in 30 μL differentiation medium without LIF. Using a micro- multi-channel pipette, the arrays of the micro drops were pipetted onto the lid of a culture dish. The lid was inverted and placed on the culture dish, which contained 5 mL differentiation medium to prevent the drops from evaporating. After 2 days, the ES cells in the drops aggregated and formed EBs, which were, then, transferred to a bacterial culture dish and cultured for another 2 days for proliferation. Thereafter, the EBs were transferred onto a collagen (0.25 mg mL^{-1}) coated culture dish (P60), and differentiated under controlled conditions.

The differentiation protocol by Hamazaki and Terada[10] toward a hepatic lineage was used for both hanging drop technique and the micropatterned EB culture. On day 8, medium was replaced with medium containing fibroblast growth factor (100 ng mL^{-1}) (MP Biomedicals, Aurora, OH). On day 11, medium was replaced with medium containing hepatocyte growth factor (20 ng mL^{-1}) (MP Biomedicals, Aurora, OH). On day 14, medium was replaced with medium containing oncostatin-M (10 ng mL^{-1}) (Sigma, St. Louis, MO), dexamethasone (10^{-7} M) (Sigma, St. Louis, MO) and ITS (insulin 5 μg mL^{-1}, transferrin 5 μg ml^{-1}, selenious acid 5 ng mL^{-1}) (BD Biosciences, San Jose, CA).

ES cell patterning using PDMS stencils and cell seeding

The shadow mask was designed to produce a center–center spacing between aggregates of 5 mm. This was to eliminate the possibility of cell interactions between the aggregates. The number of aggregates in an array was 25 (5 × 5). Photosensitive epoxy (SU-8, Microchem, Newton, MA) was spun-coated onto the silicon wafers which had been cleaned with oxygen plasma. The thickness of SU-8 was approximately 100 μm. The wafers were then soft baked at 65 °C for 5–20 min, followed by pre-baking at 100 °C for 20–90 min, depending on the thickness of the SU-8. The wafers were exposed to UV light (360 nm wave length) through the shadow mask, followed by post-exposure baking at 100 °C for 10–20 min. The SU-8 patterns on the substrates were developed in SU-8 developer (Microchem, Newton, MA) for 10 min and rinsed with IPA (isopropyl alcohol) three times. After drying the substrates using nitrogen gas, they were over-exposed to UV-light without a mask and baked at 150 °C for 1 h. Poly-dimethylsiloxane (PDMS) (Sylgard 184, Dow Corning, Midland, MI) was mixed with curing agent (10 : 1 ratio), and poured on the wafers after degassing bubbles entrapped in the PDMS mixture. On the applied PDMS, a polyacetate film was placed and clamped with an aluminium block, making the plastic film contact the top surface of the SU-8. The PDMS and aluminium block were heated to 90 °C for curing for 12 h. The next day, the PDMS stencil was detached, trimmed and sterilized in ethanol for 20 min for cell patterning (Fig. 1A). Rat tail collagen (type I) diluted in water (0.25 mg mL^{-1}) was applied and incubated overnight on tissue culture grade dishes (60 mm). The excess collagen water mixture was aspirated, and dried in a laminar flow hood. The PDMS stencil was then attached to the culture dish surface (Fig. 1B). ES cells were seeded at a concentration of 0.5 × 10^6 cells mL^{-1} in 2 mL culture medium with the stencil attached. Cells immediately began to aggregate, even as early as one hour after seeding. Detaching the stencil on day 2 after seeding ES cells allowed for stable aggregate formation (Fig. 1C). If the stencil was detached after day 2, the cells proliferated and continued to grow up vertically to the height of the stencil itself, and the detachment of the stencil became difficult without disrupting the pattern.

After the stencil was removed on day 2, the average diameters of the micropatterned aggregates and EBs were measured by Sigmascan Pro image software (Jandel Scientific, CA). Once the stencil was removed, the ES cells would migrate out of the aggregates and form outgrowths. The phase-contrast images demonstrate that these cells can form outgrowths, and the aggregates remained for 18 days of culture with uniform spacing and at uniform size. Compared to other studies,[10,17,31] our protocol does not need a suspension stage in the formation of aggregates. For monolayer culture, ES cells were seeded in collagen-coated culture dishes (60 mm) at a concentration as low as ~1000 cells mL^{-1} in 2 mL of culture medium to prevent cell–cell interaction.

Immunofluorescence assay

Primary antibodies for intracellular staining were rabbit anti-*β-III tubulin* (Chemicon, Temecula, CA), mouse anti-*Muscle specific actin* (Lab Vision, Fremont, CA), and goat anti-*AFP* (Santa Cruz Biotechnology, Santa Cruz, CA) with 1 : 200 dilution. Secondary antibodies were anti-goat, rabbit, or mouse IgG conjugated with FITC or Cy3 (MP Biomedicals, Aurora, OH). The samples were washed twice with phosphate-buffered saline (PBS) and fixed in 4% paraformaldehyde in PBS at room temperature for 30 min. After incubation, the dishes were washed twice in PBS, followed by adding 0.2% Triton X-100 in PBS to permeabilize cells for intracellular

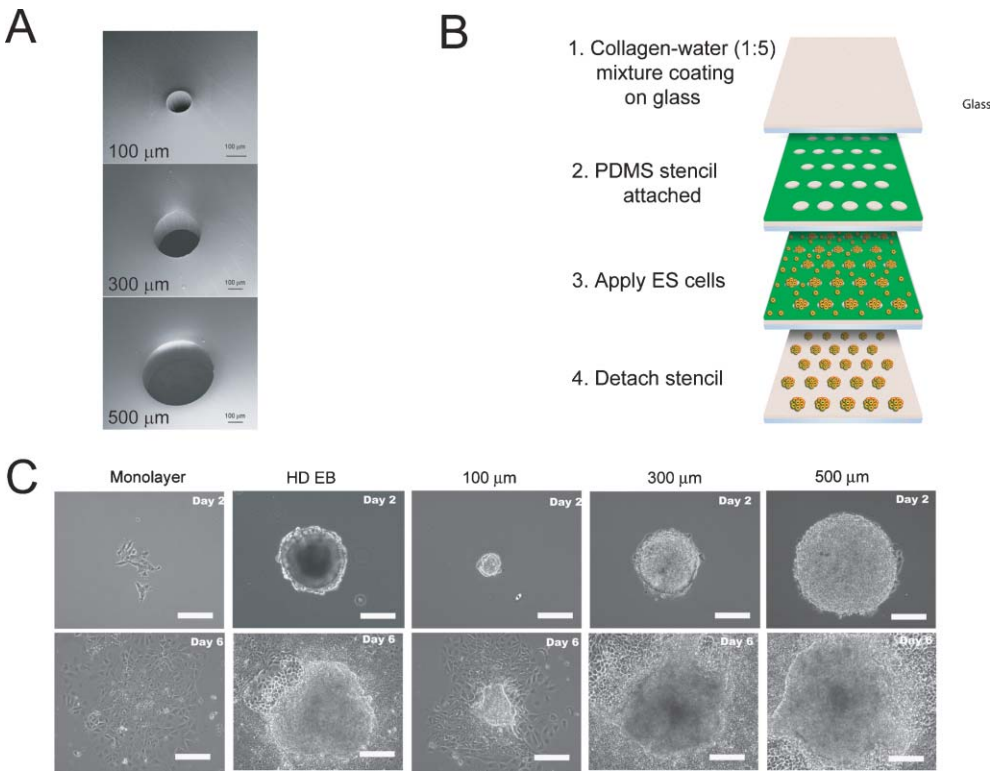

Fig. 1 (A) SEM (scanning electron microscope) images of microfabricated stencils of 100, 300, 500 μm diameter. The thickness of the stencils was kept uniform at approximately 100 μm. (B) Schematic for patterning ES cells. The PDMS stencil was attached on a collagen-coated glass, and ES cells were seeded with 0.5×10^6 cells mL^{-1} in 2 mL. Initially, ES cells were seeded in each well as a confluent monolayer. By day 2, the ES cells proliferated and formed an array of aggregates. When the PDMS stencil was detached, the aggregates remained attached on the collagen-coated surface. (C) Phase-contrast photomicrographs of patterned ES cell aggregates on day 2.

staining. After a 5 min incubation at room temperature, the cells were washed twice in PBS and resuspended in blocking buffer (PBS/20% FBS/0.05% Triton X-100) to block non-specific antibody binding, and then incubated for 60 min at room temperature. The primary antibodies were added and incubated for 2 h at room temperature. After washing twice in blocking solution, cultures were incubated with the secondary antibody FITC or Cy3-conjugated rabbit, mouse, or goat IgG for 60 min at room temperature, and washed twice at room temperature. In some cases, cells were counter-stained with 4′,6-diamidino-2-phenylindole (DAPI) (Invitrogen, Carlsbad, CA) for nuclear staining. The immunofluorescence images were obtained by using a Zeiss Microscope. Since the central core of the aggregates and EBs showed non-specific staining, the images were therefore obtained from the peripheral area.

Functional analysis (albumin and urea assays)

The culture medium samples were collected for analysis of albumin and urea content. The albumin content was determined by enzyme-linked immunosorbent assay (ELISA) using purified mouse albumin and a peroxidase-conjugated antibody (Bethyl Laboratory, Montgomery, TX, USA). Urea content was determined with a commercially available kit (StanBio Laboratory, Boerne, TX, USA). Standard curves were generated using purified mouse albumin or urea dissolved in culture medium. Absorbances were measured with a Thermomax microplate reader (Molecular Devices, Sunnyvale, CA, USA).

Reverse transcript PCR

Differentiated cells were collected by using trypsin/EDTA and cell scraper. Typically, the number of the collected cells was more than 10^6. RNA isolation was performed using the Nucleospin II RNA kit according to manufacturer's instructions. Isolated RNA typically demonstrated a ratio of A260/A280 $\geqslant$ 1.8. One-Step RT-PCR kit from Qiagen (Qiagen, Valencia, CA) was used for PCR. For each RNA isolation, RNA gel was performed. Reaction conditions for all genes were based on the manufacturer's instructions. Primers were designed using the Primer 3 Software available on the Web (http://frodo.wi.mit.edu/cgi-bin/primer3/primer3_www.cgi). RNA (10 ng) was added for each reaction condition, and primer concentrations were calculated to be 0.6 nM. The primers are listed in Table 1. Cycling conditions for three-step cycling were: denaturation at 94 °C for 30 s, annealing at 55 °C for 30 s, and extension at 72 °C for 1 min. The number of cycles varied between 30 and 35, so as not to saturate the reaction. A final extension time of 10 min at 72 °C was also performed. Following PCR, samples were run on 2% agarose gel, and labeled with ethidium bromide solution. The gels were imaged using a Fluor-X Multiimager (Bio-Rad Laboratories, Hurcules, CA). For better comparison, the gel images were quantified by using Quantity One (Bio-Rad). The reading was

Table 1 Oligonucleotide primers

Marker	Description	Primer	Sequence (5′–3′)
β-Actin	House Keeping Gene	L	GAGGGAAATCGTGCGTGA
		R	CCAAGAAGGAAGGCTGGAA
Foxa2	Endoderm	L	ACACGCCAAACCTCCCTAC
		R	GGGCACCTTGAGAAAGCA
AFP	Endoderm	L	AACTCTGGCGATGGGTGTT
		R	AAACTGGAAGGGTGGGACA
Alb	Endoderm	L	CCCTGTTGCTGAGACTTGC
		R	TGAGGTGCTTTCTGGGTGT
Sox17	Endoderm	L	ATCCAACCAGCCCACTGA
		R	TCGGCAACCGTCAAATG
Sox7	Visceral Endoderm	L	GACCAGCCTCATCTCAGTCC
		R	TTTGACCTCTTGCCAA
Foxf1	Mesoderm	L	CGTGTGTGATGTGAGGTGAG
		R	CTCCGTGGCTGGTTTCA
GATA1	Mesoderm	L	CACCATCAGGTTCCACAGG
		R	TTGAGGCAGGGTAGAGTGC
Nkx2.5	Mesoderm	L	CGTCCAACCCACACAAAC
		R	TTGTCTTCCGCTGTGTCC
Ascl1	Ectoderm	L	AAC AAACCAGACAGCCAACC
		R	TGTGACGCTCTT GCTCCA
HES1	Ectoderm	L	TGGGTCCTAACGCAGTGTC
		R	GTGAGAAGAGAGAGGTGGGCTA
Ngn2	Ectoderm	L	GCAGGCAGTTCGTGTGAA
		R	GCAATGGGAATAGAGCAGATG

based on the average of the product of the intensity. The background intensity at the outside of each band was read orthogonally to the direction to the band migration, and was subtracted from the intensity of the band. Finally, this subtracted intensity was normalized with respect to the reading of the brightest band in each gene. This semi-quantitative PCR has a limitation that the intensity reading is meaningful only when the RT reaction is not saturated. To address this limitation, we adjusted the number of cycles ranging from 30 to 35. Also, to make it possible to compare a specific gene expression level properly, all samples after PCR were migrated in the same gel.

Results

Germ layer differentiation varies with initial size of aggregate

Using the microfabricated stencil technique as a tool to study differentiation, we varied the diameter of the holes in the stencil to investigate the effect of the initial size of the aggregate on late stages of differentiation of three germ layers. The diameters of the stencil holes were 100, 300, and 500 μm (Fig. 1A). The actual sizes of the patterned aggregates after stencil removal were measured on day 2. Compared to the hanging drop EBs (SD = ± 65.8 μm, N = 8), the patterned aggregates showed much less variation in size (SD = ± 15.3 μm, N = 24). In terms of the aggregate size, the 300 μm diameter aggregates were similar to the EBs made using the hanging drop technique (Fig. 1C).

To establish baseline conditions of germ layer expression, we investigated and compared the fate of the ES cells in EBs and single ES cells plated in a monolayer configuration by using PCR and immunofluorescence assays to assess germ layer differentiation. In the EB culture, transcripts for all germ layers, mesodermal (Fig. 2A), ectodermal (Fig. 3A), and endodermal (Fig. 4A) genes were present. For the monolayer condition, transcripts for endoderm and mesoderm were present, but no transcript for ectoderm was present. This PCR result was consistent with immunofluorescence image data, showing that *muscle-specific actin* (mesoderm) (Fig. 2C), *β-III tubulin* (neuroectoderm) (Fig. 3C) and *AFP* (endoderm) (Fig. 4C) were positive for EBs. For the monolayer condition, the immunofluorescence data showed that *AFP* was expressed in a significant fraction of the cells, *muscle-specific actin* was expressed in small clusters, and *β-III tubulin* was expressed very weakly. These results show that EBs and monolayer cultures were not only morphologically different, but also different in differentiated lineages.

To measure mesodermal differentiation in the micropatterned ES cell aggregates, we measured the presence of major regulatory transcription factors, *Nkx2.5* (cardiac mesoderm), *Foxf1* (mesenchymal mesoderm) and *GATA1* (hematopoetic and endothelial). *Foxf1* was not detected in ES cells patterned in the 100 μm aggregates but was detected in ES cells patterned in 300 μm and 500 μm aggregates (Fig. 2A, B). This supports the fact that mesenchymal phenotypes varied with the size of the aggregate. *GATA1* expression was low but similar in the 100 and 300 μm aggregates, while higher in the 500 μm aggregates, indicating that hemangioblast and/or hematopoietic induction was favored in the larger aggregates. However, both *Foxf1* and *GATA1* expressions in the aggregates were lower than in the monolayer culture (Fig. 2B). Interestingly, a significant difference was seen in the marker *Nkx2.5*. This marker was strongly expressed in the 300 μm case with decreased expression in the 500 μm case, and was very weakly expressed in the 100 μm case. Thus, mesenchymal phenotypes as well as cardiac mesoderm marker Nkx2.5 were favored in the 300 μm and 500 μm aggregates, while the mesodermal phenotypes were downregulated in the 100 μm aggregates. For the immunofluorescence assay, *(smooth) muscle-specific actin* was stained and showed a similar trend as *Nkx2.5* gene expression (Fig. 2C). Taken together, these results showed that mesenchymal and hematopoietic mesoderm were favored in the monolayer culture and the larger initial aggregate size, while cardiac mesoderm was favored in the 300 and 500 μm aggregates.

It has been shown that multiple *bHLH* genes play a critical role in the regulation of neural stem cell differentiation.[34] In order to measure neural differentiation, we focused on three critical transcription factors that represent early neural commitment and/or early differentiation. For example, it is known that *HES* genes regulate maintenance of neural stem cells, while *Ascl1 and Ngn* promote neurogenesis.[35] Thus we chose to measure *Ascl1*, which is a proneural transcription factor that specifies cortical neurons.[35] In addition, we measured *HES* genes, and *Ngn2*, which specifies neural progenitors with glutaminergic receptors.[34] The hanging drop EBs expressed *HES* and *Ascl1*, while *Ngn2* was less expressed (Fig. 3A). For the 100 μm aggregates, *HES1* was expressed positive, while *Ngn2* and *Ascl1* were less expressed, compared to the hanging drop EBs, respectively (Fig. 3A, B). At the intermediate aggregate size of 300 μm, all three markers were clearly expressed. ES cells in 500 μm aggregates did not express any neural markers, similar to ES cells cultured in a monolayer

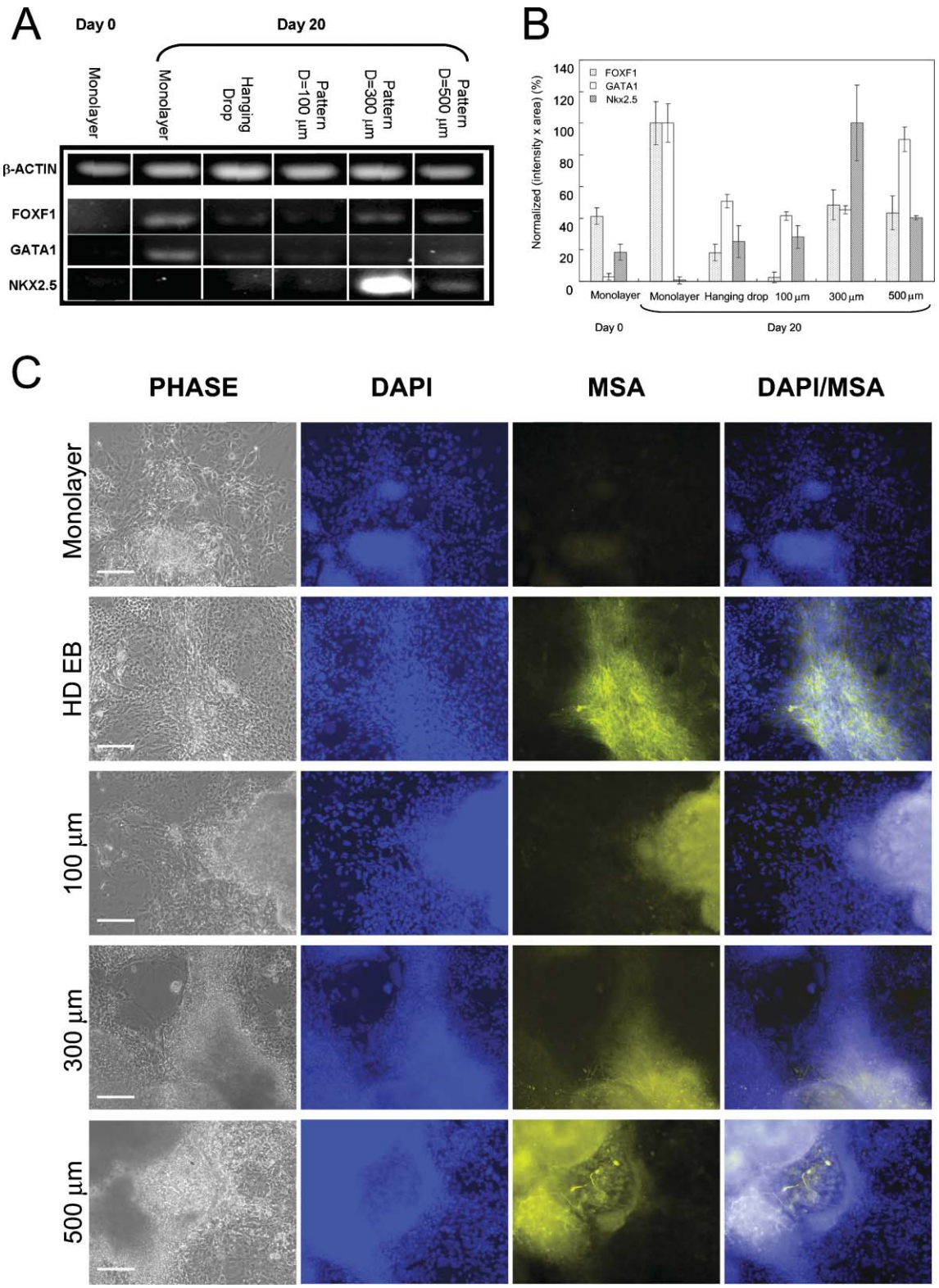

Fig. 2 Mesoderm differentiation of the patterned aggregates. (A) PCR gel images for mesoderm markers. (B) Quantified relative expression levels of each gene, based on area and intensity. The product of area × intensity, from which the background was subtracted, was normalized to the maximum value for each gene, (C) Immunofluorescence images of *muscle-specific actin*. Scale bar = 150 μm.

(Fig. 3A, B). An immunofluorescence assay was also performed for *β-III tubulin*, which is specific for neuronal differentiation, which is developed at late stage differentiation. Accordingly, *β-III tubulin* showed the strongest expression in the 300 μm aggregates (Fig. 3C). Taken together, these results suggest that *HES1* progenitors existed in the 100 μm and 300 μm case, but that a fraction of these were more differentiated into *Ascl1*+ and *Ngn*+ populations in the

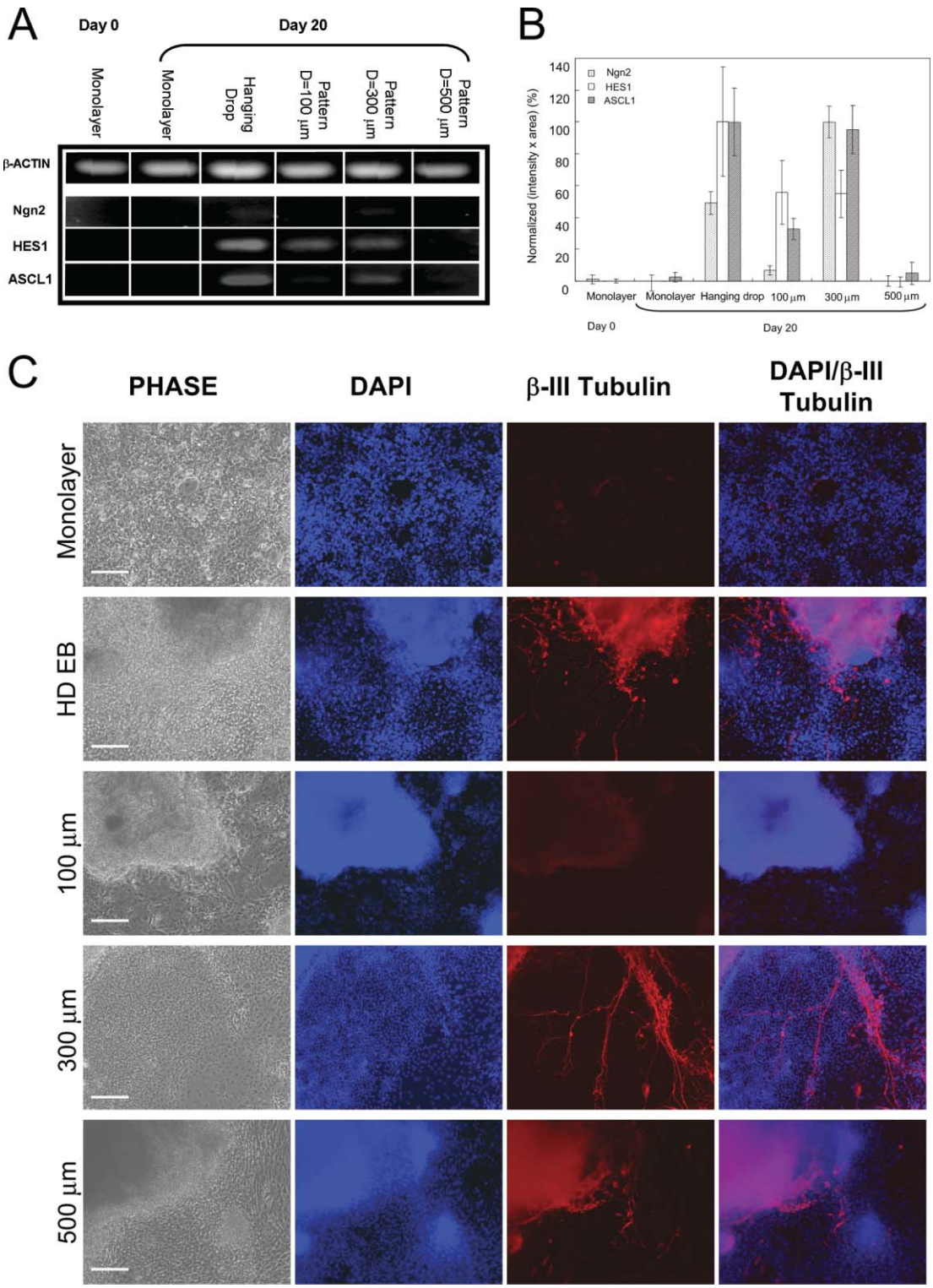

Fig. 3 Ectoderm differentiation of the patterned aggregates. (A) PCR gel images for ectoderm markers. (B) Quantified relative expression levels of each gene, based on area and intensity. The product of area × intensity, from which the background was subtracted, was normalized to the maximum value for each gene. (C) Immunofluorescence images of *β-III tubulin*. Scale bar = 150 μm.

300 μm aggregates. In the 500 μm case, it appears that neuronal differentiation was very limited.

The endoderm gives rise to many lineages, and thus far it has been the most difficult germ layer to induce and differentiate.[36] In this case we chose to expand the endoderm lineage using a known protocol, initially reported by Hamazaki and Terada.[10] The major factors agreed upon include *Foxa2* and *Sox 17*[37] which are regulatory transcription factors coexpressed in definitive endoderm. The visceral endoderm, a derivative of extraembryonic endoderm, which many times can also be

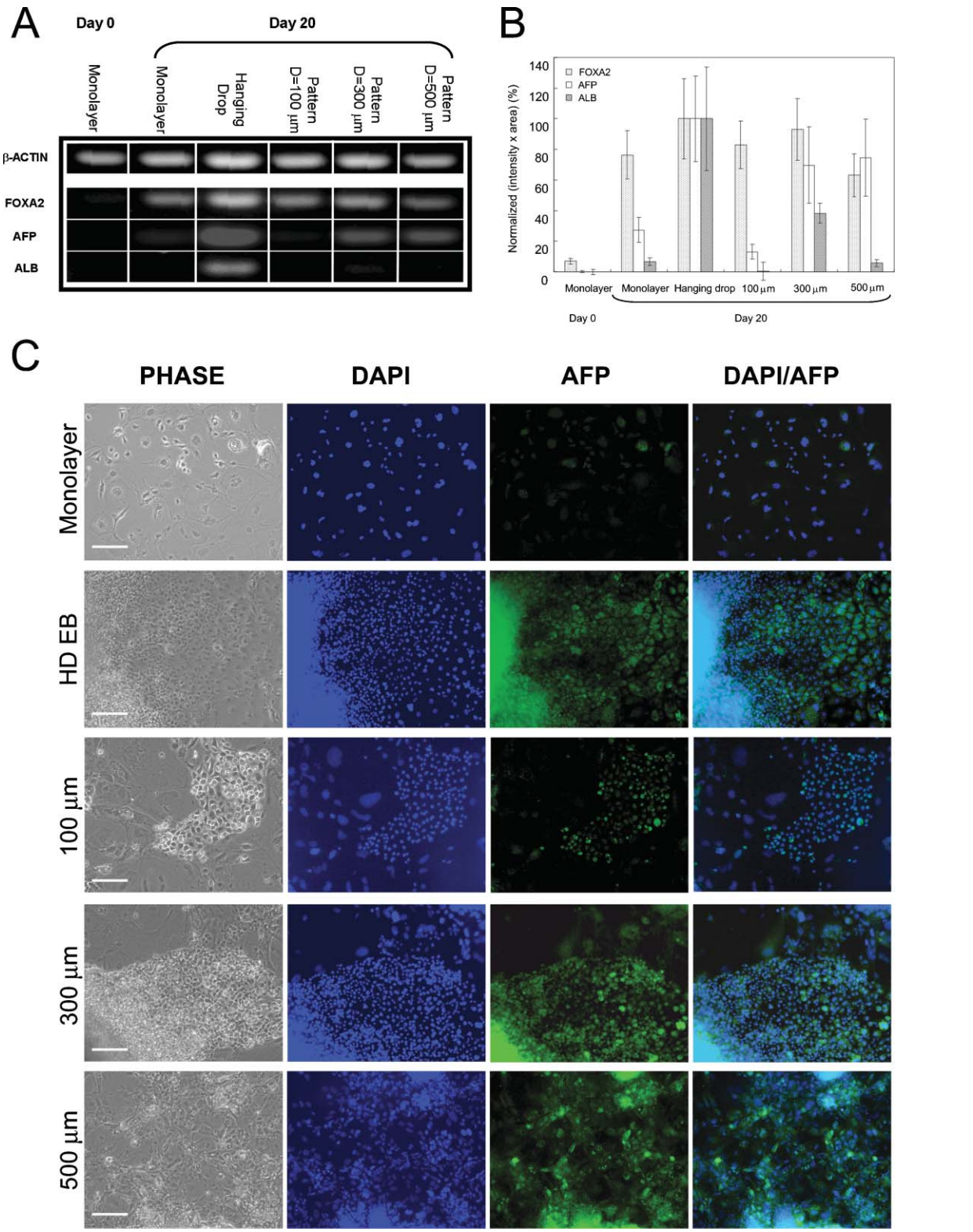

Fig. 4 Endoderm differentiation of the patterned aggregates. (A) PCR gel images for endoderm markers. (B) Quantified relative expression levels of each gene, based on area and intensity. The product of area × intensity, from which the background was subtracted, was normalized to the maximum value for each gene. (C) Immunofluorescence images of *AFP*. Scale bar = 150 μm.

generated in endoderm differentiation protocols, and also coexpresses *Foxa2* and *Sox17*, was measured using *Sox7* expression.[38] We chose to measure the extent of liver differentiation by measuring *Foxa2*, *AFP* and *Albumin* (*Alb*) gene expression, which when coexpressed, signifies activation of the liver program *in vivo*.[39] When we varied the size of initial

aggregate and measured markers for endoderm, *Foxa2* was positive for all sizes, suggesting that early endoderm-like progenitors were present (Fig. 4A, B). However, *AFP*, a marker for late endodermal and early hepatic expression, was significantly lower in 100 μm aggregates compared to 300 μm or 500 μm aggregates, suggesting that these cells had not undergone endodermal differentiation even by day 20. *Alb*, a marker for commitment to the hepatic lineage, was only expressed in the 300 μm aggregates and not in the 100 μm and weakly expressed in the 500 μm aggregates. This suggested that only the 300 μm aggregate promoted hepatic differentiation. For the immunofluorescence assay, *AFP* expression was weak in ES cells cultured in monolayers or 100 μm aggregates, while strong in 300 and 500 μm aggregates, and hanging drop EBs (Fig. 4C). These results demonstrated that the extent of endoderm differentiation varied from the least at 100 μm, to intermediate at 500 μm, and most at 300 μm, indicating that there was an optimal aggregate size for endoderm differentiation.

Micropatterned aggregates demonstrate similar differentiation kinetics

Screening of the germ layer markers while varying the size of initial aggregate demonstrated that the size of the micropatterned aggregates could contribute to germ layer formation. To further assess how well micropatterned aggregates differentiated compared to EBs made using the hanging drop technique, we examined both the kinetics of gene expression as well as a functional assay. We focused analysis to endoderm induction and differentiation, using the Hamazaki protocol.[10] We also chose the aggregate condition of 300 μm because its size and gene expression profile closely mimicked those of the EB. In addition to *Foxa2*, *AFP* and *Alb* which were previously measured, we also compared *Sox 17* which is a regulatory transcription factor coexpressed in definitive endoderm, and Sox7 which is expressed in the visceral endoderm.[37,38] Gene expression studies indicated very similar kinetic profiles for the EB and the 300 μm aggregate. Fig. 5A and B show the gene expression profiles of endoderm and mesoderm markers on culture days 10 and 20. As can be seen, transcripts for *Foxa2*, *Sox17, Sox7, and AFP* were expressed in both the EB and the micropatterned aggregates on day 10. On day 10, *Alb* was not expressed in the EB or the micropatterned aggregate conditions. This suggests that both conditions made the same amount of endoderm progenitor cells. By day 20, there was an up regulation of *Alb* in both the EB and the micropatterned 300 μm aggregate conditions. This indicated that the endoderm had been specified towards liver. Hamazaki and Terada[10] reported that hepatic differentiation was observed using hanging drop EBs and urea synthesis was detected. We also examined urea and *Alb* secreted in medium, which are specific for hepatocyte-like cells and have been used as functional markers in hepatocyte studies (Fig. 5C). The EB and the micropatterned aggregates demonstrated similar urea function, 6.75 and 6.27 μg mL^{-1} on day 11, 4.45 and 5.86 μg mL^{-1} on day 14, and 5.69 and 5.41 μg mL^{-1} on day 16 of culture, respectively. However, *Alb* secretion could not be detected in the EBs or in the micropatterned aggregates, possibly due to a shorter duration of differentiation or a different protocol, compared to He *et al.*[17]

We also examined Oct-4 expression kinetics in the microfabricated aggregates and the EBs. Oct4 is a regulatory transcription factor that is a major regulator of pluripotency, and is down regulated when the ES cells begin to differentiate. The ES cell line we used to probe Oct4 expression had the GFP protein knocked in at one allele of the Oct-4 locus. To compare the Oct4 kinetics, we used three experimental culture conditions, including micropatterned aggregates with 300 μm diameter, EBs, and monolayer culture. Fig. 5D demonstrates the conditions on culture day 2 and 10. On day 2, all three culture conditions contained ES cells expressing Oct4-GFP (Fig. 5D). In micropatterned aggregates and in the EB condition, Oct 4 expression was prominent within the aggregates. In the monolayer condition, single cells retained Oct4 expression. On day 10, the outgrowths from the microfabricated aggregates and EB condition no longer expressed Oct4. The central or "core" ES cells still expressed Oct4 in the case of micropatterned aggregates and EBs. In the monolayer, most of the cells did not express Oct-4. These results indicate that the single cells in the monolayer, which have less cell–cell contact, differentiated faster, compared to the micropatterned aggregates or EB cultures. In contrast, the Oct-4 expression of the micropatterned aggregates was similar to that of the EB culture.

In summary, the studies of gene expression kinetics and the functional studies suggest that similar rates of differentiation occurred in both EBs and the 300 μm aggregates, suggesting that the "normal" mechanisms of differentiation due to aggregation were present in the micropatterned 300 μm aggregates.

Discussion

ES cell differentiation has been known to depend on many different culture conditions, such as ECM,[26] growth factors,[12–14] local oxygen concentration,[40–42] and cell–cell interactions.[43,44] Given that ES cells form aggregates during differentiation, direct physical contact among ES cells in an aggregate plays an important role in differentiation. These interactions can be modulated in several ways. By controlling the size of the ES cell aggregate, we focused on the effects of initial aggregate size on differentiation. Using hanging drop or suspension culture methods,[11,43] it is not easy to control the initial size of the aggregates. Our study demonstrated that the EBs generated in the hanging drop method had a large variation in size. It has also been shown that the attachment efficiency of EBs depends on the oxygen concentration which is also an important differentiation factor.[40,42] This poor control of initial conditions of ES cells makes exact characterization of differentiation difficult. Instead of forming EBs in suspension, Konno *et al.* seeded ES cells directly on a hydrophobic polymer surface and formed EBs on the surface.[20] They found that the size of the EBs depended on the initial number of the seeded cells. However, it has been reported that this method of EB formation resulted in differentiation limited to the neural lineage. We demonstrated that by using the microfabricated stencils, the initial size of the

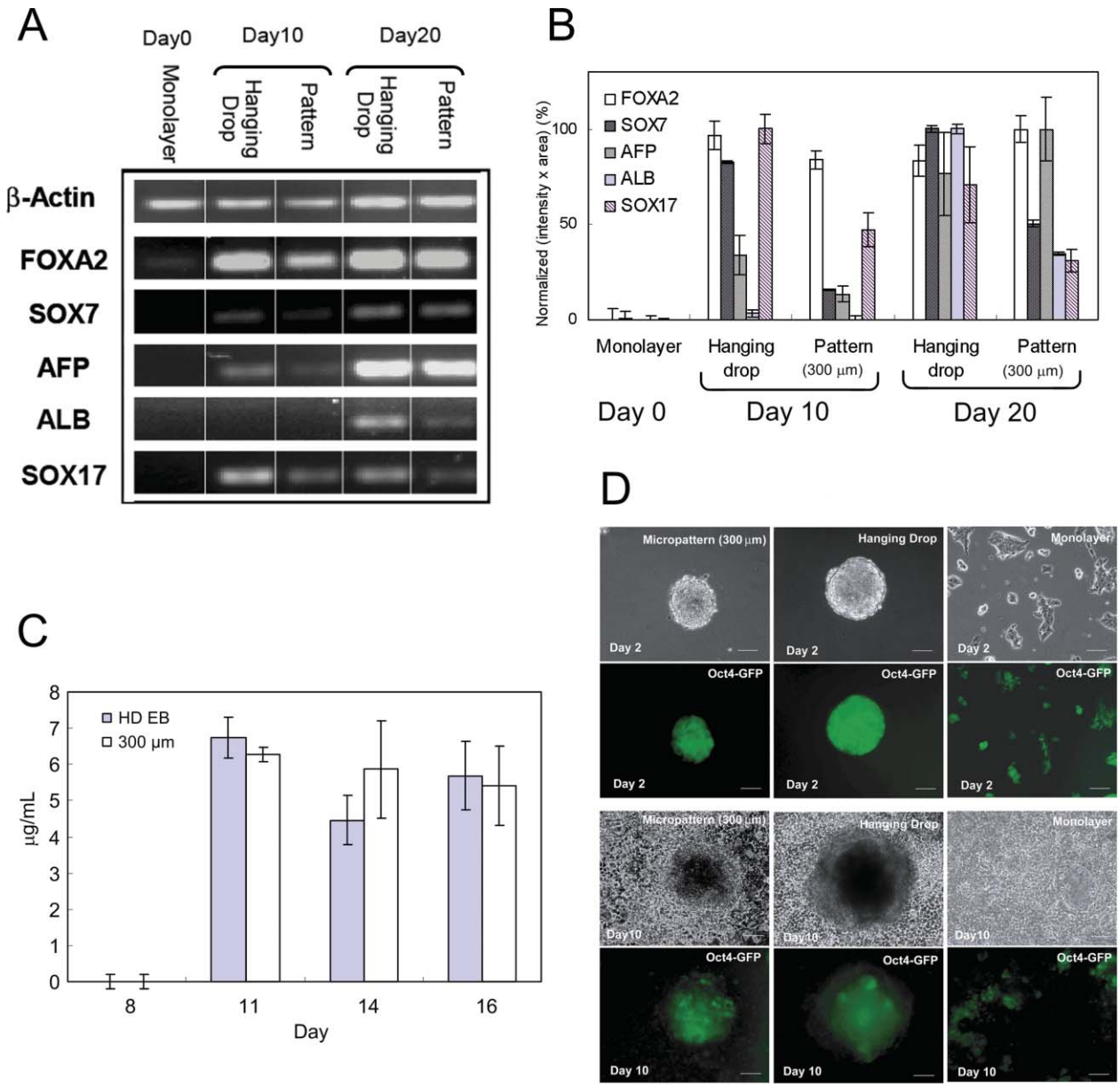

Fig. 5 Comparison of the kinetics of endoderm differentiation in EBs and the 300 μm aggregates. (A) PCR gel images for endoderm markers. (B) Quantified expression levels. (C) Urea synthesis rates. (D) Oct4-GFP signal intensity was compared among the patterned 300 μm ES cell aggregate, the hanging drop EB and single ES cells in monolayer on day 2 of culture. Both the 300 μm aggregate and the EB had a GFP+ primitive core at the center, while single ES cells in the monolayer were mostly GFP- after 10 days of culture. Scale bar = 100 μm.

aggregates could be precisely controlled. By controlling the aggregate size using the microfabricated stencils, we could easily create aggregates over a 2 day period which is similar to the time typically reported, using hanging drop technique or suspension culture. The stencil technique offers increased ability to control the shape and size of the aggregate.

Using the micropatterning method, we found that the micropatterned ES cell aggregate with 300 μm diameter, which was approximately the same size as the hanging drop EB, showed very similar differentiation profiles to those of the hanging drop EBs, while the smaller and larger aggregates showed different differentiation profiles. The 100 μm aggregates showed the stronger expression of ectodermal markers than the 500 μm aggregates, while the 500 μm aggregates showed the stronger expression of mesodermal and endodermal markers than the 100 μm aggregates. However, the 300 μm aggregates showed the strongest markers for all germ layers compared to the other patterned aggregates, except for mesenchymal (*Foxf1*) and hematopoietic (*GATA1*) mesodermal differentiation which were strongest in the monolayer culture. There could be several possible explanations for this phenomenon. As the size of the aggregate changes, the cells will experience different microenvironments. One mediator for cell–cell contact for ES cell differentiation is cadherin. Cadherins comprise a family of Ca^{2+}-dependent cell adhesion molecules which generally interact with each other

homophilically. Larue *et al.* performed a comparative study of the effect of E-cadherin on differentiation.[45] When injecting cadherin-/- ES cells into blastocysts to analyze their ability to participate in the formation of the chimeric embryos, they found that E-cad-/- ES cells contributed very poorly to chimera, most likely due to their deficiency in cell adhesion, indicating that E-cadherin is required for early cell condensation, which might be a prerequisite for subsequent inductive events leading to controlled cell patterning and the generation of differentiated structures. In addition, as ES cells differentiate, E-cadherin expression is downregulated,[46] hindering cell aggregation.[47] In our study the single cells in the monolayer had less contact with neighboring cells, compared to the cells in the aggregates where E-cadherin is expressed, possibly inducing different differentiation. Also, when the initial aggregate size was small, such as 100 μm, the cells in the aggregates differentiated faster. This fast differentiation is shown in the monolayer (Fig. 5D). These differentiated cells may lose E-cadherin expression,[46,47] resulting in the differences seen in differentiation.

While E-cadherin is fixed on the membrane, soluble factors can diffuse between cells. As the size of the ES cell aggregate changes, the mass transport rate by diffusion through the tissue will be different, and the local concentration of exogenous and autocrine factors as well as metabolites will be different. For example, when the size of the aggregate is small, it may be difficult to localize autocrine factors. This effect can be applied to many molecules, since ES cells secrete morphogens, FGF, Activins and Wnts, which form gradients in an aggregate and help promote specification of specific cell fates at an early stage of differentiation.[37,48,49] In contrast, exogenous factors for specific differentiation as well as nutrients can be supplied easily in small aggregates.

Although the aggregate with 300 μm diameter showed similar differentiation as the EBs, there was a slight difference between them. Coucouvanis and Martin[50] demonstrated that EB lumen formation occurred as a result of inward apoptosis signals from visceral endoderm on the outer surface of the EB, and also showed that an extracellular matrix signal may provide survival signals for ectodermal cells lining the lumen, thereby disrupting the patterning during differentiation. That means that these apoptosis and survival signals can be disrupted as the initial three-dimensional geometry of the micropatterned aggregate changes. Visceral endoderm has been known to form on the surface of suspended EBs. The fate of the cells attached on the extracellular matrix in the aggregate was not clear. This fate uncertainty may disturb the inward apoptosis signal and cause the slight difference in differentiation seen between the suspended EBs and the 300 μm diameter aggregates.

One interesting observation is that when the spacing between the aggregates was small (1.5 mm), the aggregates interacted. We suspect this interaction may affect cell differentiation. To study the effect of the aggregate size, we eliminated this interaction by providing enough spacing (5 mm) between the aggregates. However, it will be interesting to study the effect of the aggregate–aggregate interaction on differentiation.

Conclusion

In this study, we introduced a microfabrication technique to study ES cell differentiation. With this technique, we characterized the differentiation of various sizes of micropatterned ES cell aggregates. We found that the differentiation of ES cells depends on the size of the aggregate, and the initial size is a critical factor controlling late stage differentiation. Among the various sizes of the micropatterned aggregates, the 300 μm diameter showed a very similar differentiation profile to the hanging drop EB, without the restriction of certain lineages which has been observed in other ES cell differentiation methods, that utilize cell attachment to a substrate. This method can be useful to study ES cell differentiation due to its ability to precisely control the size of the aggregates.

Acknowledgements

This work was partially supported by grants from the National Institutes of Health (K08 DK66040 and R01 DK43371) and the New Jersey Commission on Spinal Cord Research. The microfabrication was performed at the BioMicroElectroMechanical Systems (BioMEMS) Resource Center at the Massachusetts General Hospital funded by the National Institutes of Health (P41 EB02503).

References

1 A. Smith, *Curr. Biol.*, 1998, **8**, R802–804.
2 D. Solter and J. Gearhart, *Science*, 1999, **283**, 1468–1470.
3 B. E. Reubinoff, M. F. Pera, C. Y. Fong, A. Trounson and A. Bongso, *Nat. Biotechnol.*, 2000, **18**, 399–404.
4 B. E. Reubinoff, P. Itsykson, T. Turetsky, M. F. Pera, E. Reinhartz, A. Itzik and T. Ben-Hur, *Nat. Biotechnol.*, 2001, **19**, 1134–1140.
5 S. C. Zhang, M. Wernig, I. D. Duncan, O. Brustle and J. A. Thomson, *Nat. Biotechnol.*, 2001, **19**, 1129–1133.
6 M. Schuldiner, R. Eiges, A. Eden, O. Yanuka, J. Itskovitz-Eldor, R. S. Goldstein and N. Benvenisty, *Brain Res.*, 2001, **913**, 201–205.
7 A. Bigas, D. I. Martin and I. D. Bernstein, *Blood*, 1995, **85**, 3127–3133.
8 D. S. Kaufman, E. T. Hanson, R. L. Lewis, R. Auerbach and J. A. Thomson, *Proc. Natl. Acad. Sci. U. S. A.*, 2001, **98**, 10716–10721.
9 S. I. Nishikawa, S. Nishikawa, M. Hirashima, N. Matsuyoshi and H. Kodama, *Development*, 1998, **125**, 1747–1757.
10 T. Hamazaki and N. Terada, *Methods Enzymol.*, 2003, **365**, 277–287.
11 G. M. Keller, *Curr. Opin. Cell Biol.*, 1995, **7**, 862–869.
12 T. Nakayama, T. Momoki-Soga, K. Yamaguchi and N. Inoue, *Neuroreport*, 2004, **15**, 487–491.
13 R. H. Miller, K. Dinsio, R. Wang, R. Geertman, C. E. Maier and A. K. Hall, *J. Neurosci. Res.*, 2004, **76**, 9–19.
14 P. Faloon, E. Arentson, A. Kazarov, C. X. Deng, C. Porcher, S. Orkin and K. Choi, *Development*, 2000, **127**, 1931–1941.
15 O. G. Morali, A. Jouneau, K. J. McLaughlin, J. P. Thiery and L. Larue, *Dev. Biol.*, 2000, **227**, 133–145.
16 X. L. Kuai, X. Q. Cong, X. L. Li and S. D. Xiao, *Liver Transpl.*, 2003, **9**, 1094–1099.
17 A. B. Hu, J. Y. Cai, Q. C. Zheng, X. Q. He, Y. Shan, Y. L. Pan, G. C. Zeng, A. Hong, Y. Dai and L. S. Li, *Liver Int.*, 2004, **24**, 237–245.
18 G. Kania, P. Blyszczuk, A. Jochheim, M. Ott and A. M. Wobus, *Biol. Chem.*, 2004, **385**, 943–953.
19 M. R. Koller and E. T. Papoutsakis, *Bioprocess Technol.*, 1995, **20**, 61–110.
20 T. Konno, H. Hasuda, K. Ishihara and Y. Ito, *Biomaterials*, 2005, **26**, 1381–1388.

21 V. L. Bautch, W. L. Stanford, R. Rapoport, S. Russell, R. S. Byrum and T. A. Futch, *Dev. Dyn.*, 1996, **205**, 1–12.
22 S. M. Dang, M. Kyba, R. Perlingeiro, G. Q. Daley and P. W. Zandstra, *Biotechnol. Bioeng.*, 2002, **78**, 442–453.
23 J. M. Karp, L. S. Ferreira, A. Khademhosseini, A. H. Kwon, J. Yeh and R. S. Langer, *Stem Cells*, 2006, **24**, 835–843.
24 E. S. Ng, R. P. Davis, L. Azzola, E. G. Stanley and A. G. Elefanty, *Blood*, 2005, **106**, 1601–1603.
25 D. Rudy-Reil and J. Lough, *Circ. Res.*, 2004, **94**, e107–116.
26 S. N. Bhatia, U. J. Balis, M. L. Yarmush and M. Toner, *FASEB J.*, 1999, **13**, 1883–1900.
27 J. Fukuda and K. Nakazawa, *Tissue Eng.*, 2005, **11**, 1254–1262.
28 C. S. Chen, M. Mrksich, S. Huang, G. M. Whitesides and D. E. Ingber, *Science*, 1997, **276**, 1425–1428.
29 R. McBeath, D. M. Pirone, C. M. Nelson, K. Bhadriraju and C. S. Chen, *Dev. Cell*, 2004, **6**, 483–495.
30 C. J. Flaim, S. Chien and S. N. Bhatia, *Nat. Methods*, 2005, **2**, 119–125.
31 A. Khademhosseini, R. Langer, J. Borenstein and J. P. Vacanti, *Proc. Natl. Acad. Sci. U. S. A.*, 2006, **103**, 2480–2487.
32 J. C. Mohr, J. J. de Pablo and S. P. Palecek, *Biomaterials*, 2006, **27**, 6032–6042.
33 A. Folch, B. H. Jo, O. Hurtado, D. J. Beebe and M. Toner, *J. Biomed. Mater. Res.*, 2000, **52**, 346–353.
34 R. Kageyama, T. Ohtsuka, J. Hatakeyama and R. Ohsawa, *Exp. Cell Res.*, 2005, **306**, 343–348.
35 P. Mattar, O. Britz, C. Johannes, M. Nieto, L. Ma, A. Rebeyka, N. Klenin, F. Polleux, F. Guillemot and C. Schuurmans, *Dev. Biol.*, 2004, **273**, 373–389.
36 G. Keller, *Genes Dev.*, 2005, **19**, 1129–1155.
37 A. Kubo, K. Shinozaki, J. M. Shannon, V. Kouskoff, M. Kennedy, S. Woo, H. J. Fehling and G. Keller, *Development*, 2004, **131**, 1651–1662.
38 S. Tada, T. Era, C. Furusawa, H. Sakurai, S. Nishikawa, M. Kinoshita, K. Nakao, T. Chiba and S. Nishikawa, *Development*, 2005, **132**, 4363–4374.
39 K. S. Zaret, *Nat. Rev. Genet.*, 2002, **3**, 499–512.
40 G. D'Ippolito, S. Diabira, G. A. Howard, B. A. Roos and P. C. Schiller, *Bone*, 2006, **39**, 513–522.
41 M. Gassmann, J. Fandrey, S. Bichet, M. Wartenberg, H. H. Marti, C. Bauer, R. H. Wenger and H. Acker, *Proc. Natl. Acad. Sci. U. S. A.*, 1996, **93**, 2867–2872.
42 M. Csete, *Ann. N. Y. Acad. Sci.*, 2005, **1049**, 1–8.
43 S. M. Dang, S. Gerecht-Nir, J. Chen, J. Itskovitz-Eldor and P. W. Zandstra, *Stem Cells*, 2004, **22**, 275–282.
44 A. Dasgupta, R. Hughey, P. Lancin, L. Larue and P. V. Moghe, *Biotechnol. Bioeng.*, 2005, **92**, 257–266.
45 L. Larue, C. Antos, S. Butz, O. Huber, V. Delmas, M. Dominis and R. Kemler, *Development*, 1996, **122**, 3185–3194.
46 Y. S. Choi and B. Gumbiner, *J. Cell Biol.*, 1989, **108**, 2449–2458.
47 M. S. Steinberg and M. Takeichi, *Proc. Natl. Acad. Sci. U. S. A.*, 1994, **91**, 206–209.
48 R. H. Xu, R. M. Peck, D. S. Li, X. Feng, T. Ludwig and J. A. Thomson, *Nat. Methods*, 2005, **2**, 185–190.
49 D. K. Singla, D. J. Schneider, M. M. LeWinter and B. E. Sobel, *Biochem. Biophys. Res. Commun.*, 2006, **345**, 789–795.
50 E. Coucouvanis and G. R. Martin, *Cell*, 1995, **83**, 279–287.

